







**Table 5 — CTS Test Weld Data for Plate 1B859 (50-mm thickness, 150-mm combined thickness, 0.33CE<sub>IIW</sub>)**

Weld No.	Diffusible H <sub>2</sub> mL/100 g Deposited	Welding Parameters		Weld Cooling Characteristics		Mean Weld Metal Hardness HV5	HAZ Cracking/No Cracking, C/NC	Proportion of Faces Cracked from a Total of Six
		Travel Speed, mm/min	Arc Energy, kJ/mm	$\Delta t_{800-500}$ , s	HAZ Hardness HV5 <sup>(a)</sup>			
W44	4.4	267	0.85	3.1	317–252 295	253	NC	0
W46	4.4	240	0.93	--	336–280 305	265	NC	0

(a) Presented as  $\frac{\text{max.}-\text{min.}}{\text{average}}$

**Table 6 — CTS Test Weld Data for Plate 1B405 (50-mm thickness, 150-mm combined thickness, 0.37CE<sub>IIW</sub>)**

Weld No.	Diffusible H <sub>2</sub> mL/100 g Deposited	Welding Parameters		Weld Cooling Characteristics		Mean Weld Metal Hardness HV5	HAZ Cracking/No Cracking, C/NC	Proportion of Faces Cracked from a Total of Six
		Travel Speed, mm/min	Arc Energy, kJ/mm	$\Delta t_{800-500}$ , s	HAZ Hardness HV5 <sup>(a)</sup>			
W57	4.4	282	0.78	—	362–345 350	280	NC	0
W56	4.4	259	0.93	—	367–313 347	283	NC	0
W60	1.7	513	0.8	—	362–310 340	269	NC	0
W61	1.7	559	0.87	—	358–325 340	261	NC	0

(a) Presented as  $\frac{\text{max.}-\text{min.}}{\text{average}}$

**Table 7 — CTS Test Weld Data for Plate 1B457 (50-mm thickness, 150-mm combined thickness, 0.37CE<sub>IIW</sub>)**

Weld No.	Diffusible H <sub>2</sub> mL/100 g Deposited	Welding Parameters		Weld Cooling Characteristics		Mean Weld Metal Hardness HV5	HAZ Cracking/No Cracking, C/NC	Proportion of Faces Cracked from a Total of Six
		Travel Speed, mm/min	Arc Energy, kJ/mm	$\Delta t_{800-500}$ , s	HAZ Hardness HV5 <sup>(a)</sup>			
W54	4.4	253	0.9	—	396–325 360	291	NC	0
W55	4.4	259	0.9	2.8	376–353 364	287	C	4
W63	4.4	246	0.96	2.7	418–349 373	291	C	1
W71	4.4	206	1.1	—	391–310 369	292	NC	0
W73	4.4	178	1.23	3.3	391–349 373	282	C	2
W72	4.4	165	1.32	4.4	412–358 385	277	NC	0
W58	1.7	513	0.8	2	396–349 370	283	NC	0
W59	1.7	513	0.87	—	401–296 350	298	NC	0

(a) Presented as  $\frac{\text{max.}-\text{min.}}{\text{average}}$

min of exposure. All test welds were made immediately after the block was removed from the freezer, refrigerator, or humidity cabinet. Two shielded metal arc consumables were used that produced weld metal hydrogen levels of 3.9 mL or 4.4 mL/100 g deposited weld metal when welding was performed under normal, dry conditions (Table 2). A measure of the actual deposited weld metal hydrogen with humidity-cabinet-induced surface moisture was made for the 3.9 mL/100 g deposited weld metal consumable. This was compared to the result obtained under normal, essentially dry, conditions. Two steels were evaluated using this technique, corresponding to 0.45 and 0.33 carbon equivalents.

## Results

### Hydrogen Levels

The hydrogen levels determined for each consumable are shown in Table 2. All are observed to be within the Scale D level (<5 mL H<sub>2</sub>/100 g deposited metal) in BS 5135: 1984.

The diffusible hydrogen present in the weld metal deposited on test blocks covered with humidity-cabinet-induced surface moisture was observed to be 4.9 mL H<sub>2</sub>/100 g deposited metal (Table 3). This represents an increase of 1 mL H<sub>2</sub>/100 g deposited weld metal in comparison with the previous result obtained under nominally dry conditions. Further assessment and data generation would be required to establish if this is a "real" difference. However, the value of 4.9 mL H<sub>2</sub>/100 g still conforms to the Scale D level stipulated in BS 5135: 1984.

### CTS Test Data

All CTS test weld results (without moisture contamination) are presented in Tables 4–10 for each individual steel composition. The HAZ cracking behavior is presented in Figs. 2–5. The predicted arc energy for the avoidance of hydrogen cracking, as defined by TWI nomograms for 50-mm (2-in.) thick steel/no preheat/Scale D hydrogen is also shown. (Note that the term "arc energy" describes the energy supplied by the arc, while the term "heat input" refers to the heat input into the steel being welded. The difference between the two terms is accounted for by the "arc efficiency" of the welding process. The arc efficiency of SMAW and FCAW is 80% for the purposes of the TWI scheme). The maximum HAZ hardness is recorded adjacent to each crack/no crack data point.

Cracking was seen to occur in steel 1B789 at a marginally higher arc energy

than that predicted as being safe by the TWI nomogram for a carbon equivalent of 0.43 (Figs. 2 and 5). Steel 1B704 (0.40  $CE_{IIW}$ ) showed a single cracked weld at an arc energy assumed to be safe, according to the TWI predictive scheme (Fig. 3), while steel 1B457 produced cracking in three test welds at conditions also predicted to be safe by the nomogram — Fig. 5. However, the other steels behaved in accordance with the TWI predictive scheme. Indeed, for steels 1B885, 1B859 and 1B485, which corresponded to carbon equivalents of 0.31, 0.33 and 0.37, respectively, no HAZ cracking could be produced, even when the lowest practicable arc energies (~0.8 kJ/mm) were employed.

In three steels for which a crack threshold could be established, the critical HAZ hardness at which cracking occurred (defined as the lowest value of maximum hardness in a cracked sample,  $HV_{crit}$ ) was observed to vary between 376 and 437 HV5 and generally appeared to decrease with lower  $CE_{IIW}$  — Fig. 6. However, for steel 1B704 where a single cracked weld was observed, this cracking occurred at a maximum HAZ hardness of 296 HV5.

#### CTS Test Data with Moisture Contamination

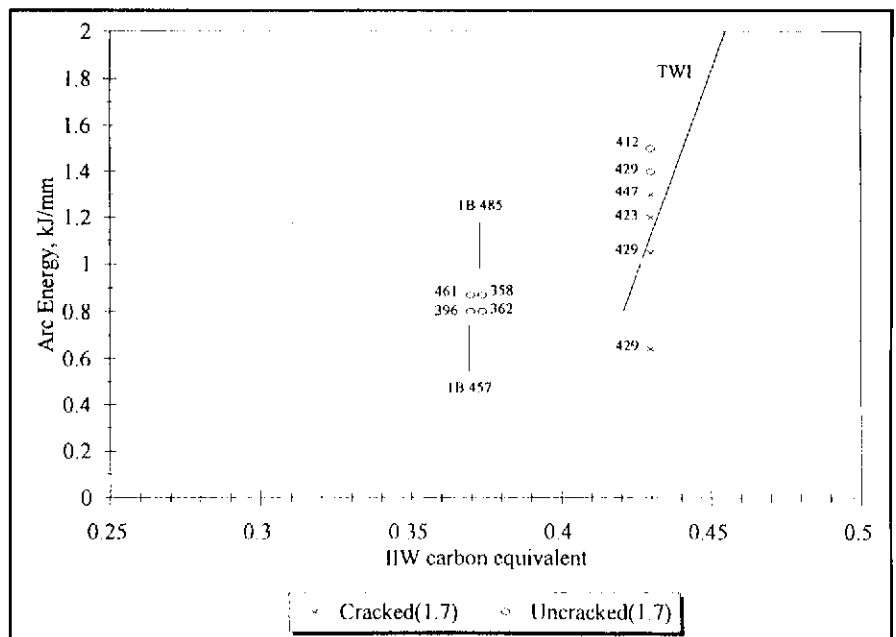
All CTS test weld results with moisture contamination are presented in Tables 11 and 12 for each steel composition examined. The cracking behavior is presented graphically in Fig. 7. The highest arc energy at which cracking was observed under dry conditions is also plotted.

For the steel of lowest carbon equivalent, 0.33 (1B859), no HAZ cracking was observed, even when consumables with a potential hydrogen level of 4.4 mL  $H_2/100$  g (when used in nominally dry conditions) were employed to weld a block covered with frost. The combination of frost, no preheat and use of the highest Scale D consumable (4.4 mL  $H_2/100$  g) constitutes the worst case examined, but cracking was not induced for the lowest practicable arc energy.

The lowest uncracked result for the CTS tests performed on steel 1B433 of 0.43  $CE_{IIW}$  was observed to be at 1.46 kJ/mm. This is ~0.2 kJ/mm higher than that observed for the same steel/consumable combination when welding was performed without contamination and does not represent a significant effect of surface moisture.

#### Metallographic Observations of Transverse CTS Test Specimens

CTS welds made by the SMAW and FCAW processes showed similar flat or convex bead surface profiles. However,





work. From consideration of the maximum hardness values obtained for a given cooling rate, it would appear that the hardenability of this steel is close to or beyond the upper bound of behavior originally introduced by Bailey (Ref. 3) into the nomogram scheme. Why this should be is not clear from the chemical analysis of the steel, but it should be noted that this steel has an untypically high niobium level for today's structural steels, and the steel also has higher carbon and lower manganese levels than are typical of many of today's structural steels. The increased hardenability associated with niobium-containing steels is accounted for in certain other carbon equivalent formulas used to assess a given steel's weldability (Refs. 12–14).

To summarize, the present CTS test work for combined thicknesses up to 150 mm has confirmed that, in general, steels with a low-carbon equivalent can indeed be welded successfully in line with TWI guidelines without the application of preheat when low-hydrogen consumables (<5 mL H<sub>2</sub>/100 g deposited weld metal) are used. The data obtained in this work consolidate the limited CTS data previously acquired at TWI for identical plate thicknesses and hydrogen levels without preheat (Ref. 15). No shortcomings in the TWI predictive scheme were highlighted by the previous work, although only two steels were investigated. It would be expected that, as the hydrogen level of the consumable is lowered, the cracking tolerance of hard heat-affected zones would increase, *i.e.*, the critical hardness for cracking would be expected to rise. Comparison of the critical hardnesses measured in the present work with those obtained for test welds deposited with Scale B (~12 mL/100 g) shown in Fig. 9 do indicate that this expected trend has been observed (Ref. 16).

#### Comparison of SMAW and FCAW Processes

Steel 1B789 produced similar crack/no-crack boundary conditions of ~1.3 kJ/mm for both the flux cored arc welds at 1.7 mL H<sub>2</sub>/100 g and the shielded metal arc welds at 4.4 mL H<sub>2</sub>/100 g, while some reduction in critical arc energy might reasonably have been expected. As was noticed earlier, the root profiles of the test fillet welds were different for both processes. The acute angle observed between the weld metal and top plate of flux cored arc welds represents an increased local stress concentration in comparison to the same region for shielded metal arc welds — Fig. 8. This may be an explanation for the absence of an improvement in the cracking risk of the lower hydrogen flux cored

**Table 9 — CTS Test Weld Data for Plate 1B789 (50-mm thickness, 150-mm combined thickness, 0.43CE<sub>IW</sub>)**

Weld No.	Diffusible H <sub>2</sub> ml/100 g Weld Deposited Metal	Welding Parameters		Weld Cooling Characteristics $\Delta t_{\text{HRC}}^{\text{WELD}}$ s	HAZ Hardness HV5 <sup>(a)</sup>	Mean Weld Metal Hardness HV5	HAZ Cracking/No Cracking, C/NC	Proportion of Faces Cracked from a Total of Six
		Travel Speed, mm/min	Arc Energy, kJ/mm					
W12	4.4	187	1.13	—	429–401 416	277	NC	0
W18	4.4	180	1.22	4.4	435–367 413	275	C	4
W19	4.4	167	1.3	5.2	423–391 412	261	NC	0
W14	4.4	173	1.32	—	418–376 402	258	C	2
W21	4.4	156	1.4	4.8	435–401 419	258	NC	0
W16	4.4	156	1.45	—	404–353 388	255	NC	0
W17	3.9	246	0.87	2.8	435–407 419	283	C	5
W15	3.9	234	0.97	—	441–388 406	257	C	6
W11	3.9	213	1.04	—	435–423 429	281	NC	0
W13	3.9	187	1.11	—	423–396 414	281	NC	0
W22	3.9	167	1.24	5	423–274 356	263	NC	0
W20	3.9	156	1.44	—	418–268 353	236	NC	0
W27	3.3	234	0.91	2.8	453–412 431	325	NC	0
W25	3.3	223	0.97	—	453–362 404	280	NC	0
W23	3.3	195	1.05	—	447–386 416	313	C	4
W33	3.3	187	1.1	—	435–310 378	286	NC	0
W31	3.3	173	1.2	4	435–371 398	275	NC	0
W29	3.3	167	1.3	—	435–407 421	277	NC	0
W36	1.7	675	0.64	—	429–295 349	338	C	6
W35	1.7	491	1.05	—	429–274 381	303	C	6
W38	1.7	—	1.2	4	423–286 371	287	C	5
W39	1.7	No data	1.3	4	447–310 368	280	C	4
W43	1.7	350	1.4	—	429–353 389	264	NC	0
W42	1.7	323	1.5	—	412–317 370	289	NC	0

(a) Presented as  $\frac{\text{max.} - \text{min.}}{\text{average}}$

arc welds relative to the shielded metal arc welds referred to above. Thus, until more data have been generated, these results suggest that some caution should be exercised when developing weld procedures for this process.

#### CTS Test Results with Moisture Contamination

Turning now to the CTS test welds that

were deposited with moisture contamination, the results are plotted in Fig. 7. Testing performed on the 1B433 (0.45 CE<sub>IW</sub>) steel showed the presence of water contamination prior to welding only shifted the crack/no-crack threshold from 1.3 kJ/mm to roughly 1.5 kJ/mm for welds deposited using Scale D consumables without preheat. This shift is within the 0.3 kJ/mm tolerance limit for threshold arc energy as defined in BS 7363:





